PAPER • **OPEN ACCESS**

Chlorinated vapor sensing performance of lipophilic calix[4]arene phosphonic acid based thin films: sensor parameters, diffusion coefficients and theoretical calculations via density functional theory

To cite this article: Inci Capan *et al* 2025 *Phys. Scr.* **100** 095403

Physica Scripta

PAPER

Chlorinated vapor sensing performance of lipophilic calix[4]arene phosphonic acid based thin films: sensor parameters, diffusion coefficients and theoretical calculations via density functional theory

Inci Capan[1,*], **Nilüfer Seda Alagöz**[1], **Mevlut Bayrakci**[2] **and Mustafa Ozmen**[3]

[1] Department of Physics, Faculty of Science, University of Balikesir, 10145, Balikesir, Turkey
[2] Department of Bioengineering, Faculty of Engineering, University of Karamanoglu Mehmetbey, 70200, Karaman, Turkey
[3] Department of Chemistry, Faculty of Science, University of Selcuk, 42250, Konya, Turkey
[*] Author to whom any correspondence should be addressed.

E-mail: ibasaran@balikesir.edu.tr **and** inci.capan@gmail.com

Keywords: calix[4]arene, spin coating, surface plasmon resonance, chlorinated VOCs, Ficks' law, density functional theory

Supplementary material for this article is available online

OPEN ACCESS

RECEIVED
19 April 2025

REVISED
13 August 2025

ACCEPTED FOR PUBLICATION
28 August 2025

PUBLISHED
10 September 2025

Abstract

A group of lower rim modified lipophilic calix[4]arene derivative with phosphonic acid groups were used to fabricate the spin coated thin films. Chlorinated volatile organic solvents; chloroform, dichloromethane and carbon tetrachloride were selected for a deep investigation of their interaction with the thin films. The thin films possessed higher affinity to dichloromethane and chloroform vapor compared with the carbon tetrachloride vapor in the manner of the physical properties of the vapor molecules such as dipole moment, refractive index, vapor pressure and molar mass. The sensor parameters; response/recovery times, reproducibility, sensitivity, limit of detection and quantification were studied via the real time kinetic interaction. Sensitivity value up to 1.29×10^{-3} ppm^{-1} was calculated where the LOD and LOQ values were obtained down to 2–3 ppm and 7–13 ppm, respectively. Response times were in the range of 1–2 s and recovery times were between 2 to 4 s for all measurements. In other respects, the kinetic data was used to adopt to the Ficks' law of diffusion model for the calculation of the diffusion constants and a two-region diffusion model was accepted where the values of the diffusion constants were found to be between $0.21–12.09 \times 10^{-15}$ $cm^2\,s^{-1}$ for the first region and $0.12–6.41 \times 10^{-17}$ $cm^2\,s^{-1}$ for the second region of the interaction. The nature of the complexation capacity was investigated via density functional theory calculations. The energy gaps between the LUMO and HOMO of calixarene complexes were calculated as 0.60 eV for carbon tetrachloride and 0.58 eV for dichloromethane complexes, whereas the energy gaps for calix-chloroform were found to be 0.51 eV, respectively. After overall assessment the highest sensing performance calix derivative was found to be **CT4PA** with four phosphonic acid groups. Theoretical data was found to be in good correlation with the experimental data.

1. Introduction

Polychloromethanes (PCMs) are a class of chlorinated volatile organic compounds (Cl-VOCs); widely used as solvents and degreasing agents which are commercially used in a variety of products can be found contaminated in soil, atmosphere and any kind of water sources including river, lakes or underground. Their use in industry in terms of in both processing and production, pharmaceuticals, dry cleaning and etc took place in human life over the past decades [1]. PCMs were reported by several studies [2–4] as the chemicals which exhibit serious health effects that could not only degenerate the liver and kidney toxicity but can also result into acute effects on the central nervous system such as depression, headache and dizziness. Members of the PCMs;

dichloromethane (CH_2Cl_2), chloroform ($CHCl_3$) and carbon tetrachloride (CCl_4) are colorless liquid volatile organic compounds at the room temperature which the threshold limit value for each of them was reported as 50 ppm, 10 ppm, and 5 ppm, respectively. They were classified in Group B which represents the possibly carcinogenicity for human According to International Agency for Research on Cancer (IARC) [5].

For the detection of the PCMs, calix[*n*]arene molecules are good candidates as macrocyclic receptors because of their bowl shaped cavitand structure. Their chemical structure facilitates to design both upper and lower rim by tailoring the favorable host structures. These functional groups provide the binding of the guest molecules via several kinds of non-covalent interactions as well as allowing the guest molecules' molecular encapsulation into their enclosed interior structure [6, 7]. Several gas sensing applications which enable to trap a variety of toxic gas molecules into the variable cavity structure at low concentrations were studied [8]. The suitable chemical structure for the fabrication of the thin films via different techniques such as self-assembly [9], Langmuir—Blodgett (LB) thin film fabrication [10] and spin coating [11] were used to analyze the calixarene layers.

The detection of the toxic volatile organic compounds (VOCs) can be made using several transduction methods such as gravimetric [12], electrical [13] or optical [14]. The Surface Plasmon Resonance (SPR) technique is a powerful technique for the detection of guest molecules by a thin film coated onto a metal thin layer. Tracking the molecular interactions in real time diagnostics with high sensitivity, ranging from cells to small molecules present advantages on the detection of the molecular binding interactions. Other optical methods however have similar abilities, SPR is the most stable and widely used technique to measure the binding kinetics, affinity and concentration of molecular interactions with its large sensing area [14–16]. SPR has distinct advantage over radioactive or fluorescent labeling methods on being cost effective [17]. Electrochemical detection equipment is simple and low cost however many target molecules do not directly transfer electrons to the electrode. Moreover, electrochemical detection is affected by electrochemical and environmental noise, therefore its sensitivity will be limited [18]. QCM sensor devices compared with the SPR sensor devices has the disadvantage of limited selectivity which depends on the availability of the coating layer [19]. The first quantitative study on the comparison of the QCM and SPR techniques was on a biosensor device similar performance was shown with parameters such as thicker functionalization layers or flow-injection apparatus design may change the results [20]. Further studies on the comparison of two techniques leaded the fabrication of simultaneous QCM/SPR chip avoiding the individual limitations of each sensor system [21] or combined use of two distinct techniques [22].

Plane polarized beam of light directed through the interface of the metal film and the dielectric thin layer is totally internal reflected at a special angle of incidence that the resonance of the plasmons occur. The excellent sensitivity of the resonance angle to the thickness and/or the optical parameters of the thin layer enables the detection of the analytes [23]. Calixarene molecules attracted great attention by the researchers whom working on SPR gas sensing decades ago, since then many studies have been carried out on this field [24]. Many volatile organic compound groups including alcohols [25, 26], aromatic hydrocarbons (BTEX) [27, 28] were studied using SPR instrument. Studies on the detection of several VOCs shown that the high sensing performance can be achieved in Cl-VOCs sensing among a number of VOCs. Previous study on the LB thin films of picoline amide based calix[4]arene shown high sensing performance to chloroform vapor among the analytes; acetone, benzene, methanol, ethyl acetate [29]. Chloroform sensing properties of LB thin films of calix[8]arenes and calix[4]arenes revealed the highest sensing ability among the other vapors; benzene, toluene and ethyl alcohol [30, 31]. The phosphonated calix[4]arene thin film which was fabricated via the LB thin film fabrication technique was exposed to chloroform, dichloromethane, carbon tetrachloride, ethanol, benzene, and toluene was found to be selective to Cl-VOCs among all analyte vapors [32]. During the preparation of smart materials, chemical modification of raw materials with phosphoric acid groups not only increases the presence of electron donor functional groups on the surface of the material but also improves thermal stability and surface acidity as well as high specific surface area and good vapor adsorption capacity. Therefore, phosphoric acid modified smart materials have promising applications in the capture of VOCs [33].

The gas sensing mechanisms and the adsorption models of the vapor molecules with the calixarene layers were studied [34, 35]. Calix[*n*]arenes ($n = 4, 6$ or 8) are an important and interesting class of macrocyclic receptors due to variety in their cavity diameters. Especially, presence of two different hydrophobic (*upper rim*) and hydrophilic regions (*lower rim*), can play an important role in the detection and early warning of pollutants in the air [8]. Calixarenes are specific and sensitive molecules for detection due to their porous structure, which allows diffusion inside the film. A large number of surface characterization techniques such as the Langmuir–Blodgett films, surface acoustic wave oscillator, and mass sensitive quartz micro balance/quartz crystal microbalance are being used with different calixarene derivatives. These techniques provides to investigate the possible interaction or association between host (calixarenes) and the guest (gas molecules) [8]. Especially, calix[4]arene derivatives which have a typical symmetrical bowl shape have attracted great interest as host molecules for both organic and inorganic guests due to their lower-edge H-bond interactions [36].

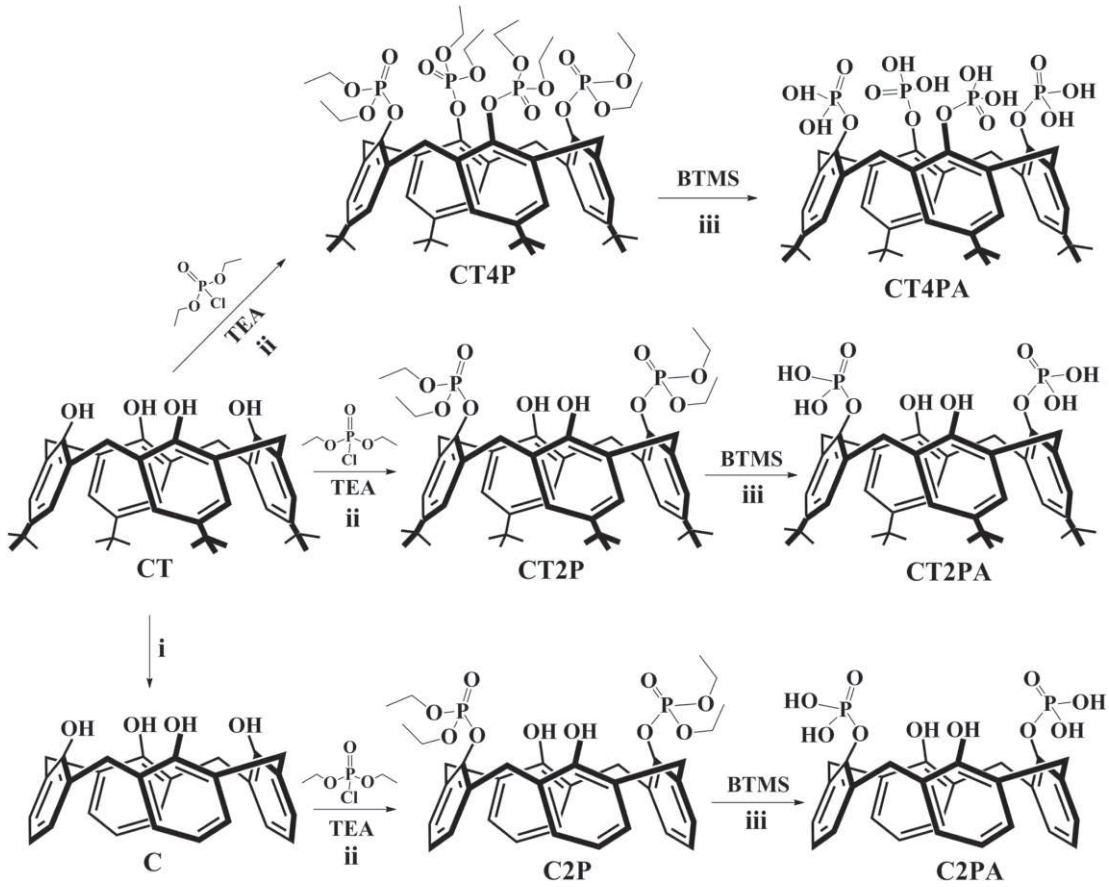

Scheme 1. Synthesis of phosphoric acid derivatives of lipophilic calix[4]arene involves the following steps: i) reaction of phenol with $AlCl_3$ in toluene; ii) treatment with triethylamine (TEA) and diethyl chlorophosphate in chloroform under reflux; iii) addition of bromotrimethylsilane in a mixture of chloroform and methanol.

In this work the spin coating thin film fabrication technique was used to fabricate the calixarene molecules onto solid substrates with different solution concentration values ranging between 1 mg ml^{-1} and 3 mg ml^{-1}. Fabrication process was controlled by UV-Visible spectra and the SPR curve investigation. The PCMs sensing properties of the calixarene thin films were investigated using the SPR instrument. The sensor parameters; Sensitivity (S), Limit of Detection (LOD), Limit of Quantification (LOQ) were calculated. The Fick's law of diffusion was utilized to analyze the kinetic data, enabling the calculation of diffusion coefficients. The nature of the complexation capacity was investigated via density functional theory calculations. Geometric optimizations and theoretical calculations of **CT4PA** and its inclusion complexes were verified by applying density functional theory.

2. Experimental

2.1. Materials and synthesis

The chemical structures of the phosphonic acid derivatives of lipophilic calix[4]arenes 25,27-Bis (diethoxyphosphonoxy)-5,11,17,23-tetra-ter-butyl-26,28-dihydroxycalix[4]arene (**CT2PA**), 25,27-Bis (diethoxyphosphonoxy)-26,28-dihydroxycalix[4]arene (**C2PA**), and 25,26,27,28-tetra (diethoxyphosphonoxy)-5,11,17,23-tetra-ter-butyl-calix[4]arene (**CT4PA**). were presented in Scheme 1. Phosphoric acid derivative of lipophilic calix[4]arene derivatives (**CT2PA**, **C2PA**, and **CT4PA**) have been synthesized from unmodified calix[4]arenes (**C** and/or **CT**). Firstly, unmodified calixarenes have been converted corresponding phosphate ester derivatives (**CT2P**, **C2P** and/or **CT4P**) with diethyl chlorophosphate in presence of triethylamine. Obtained phospho-esteryl groups of calixarene derivatives (**CT2P**, **C2P** and/or **CT4P**) have been easily hydrolyzed with bromotrimethylsilane to obtain targeted phosphoric acid derivatives of calixarenes (**CT2PA**, **C2PA** and **CT4PA**). All analytical data pertaining to their structural analysis are in excellent agreement with previously published results in the literature [37].

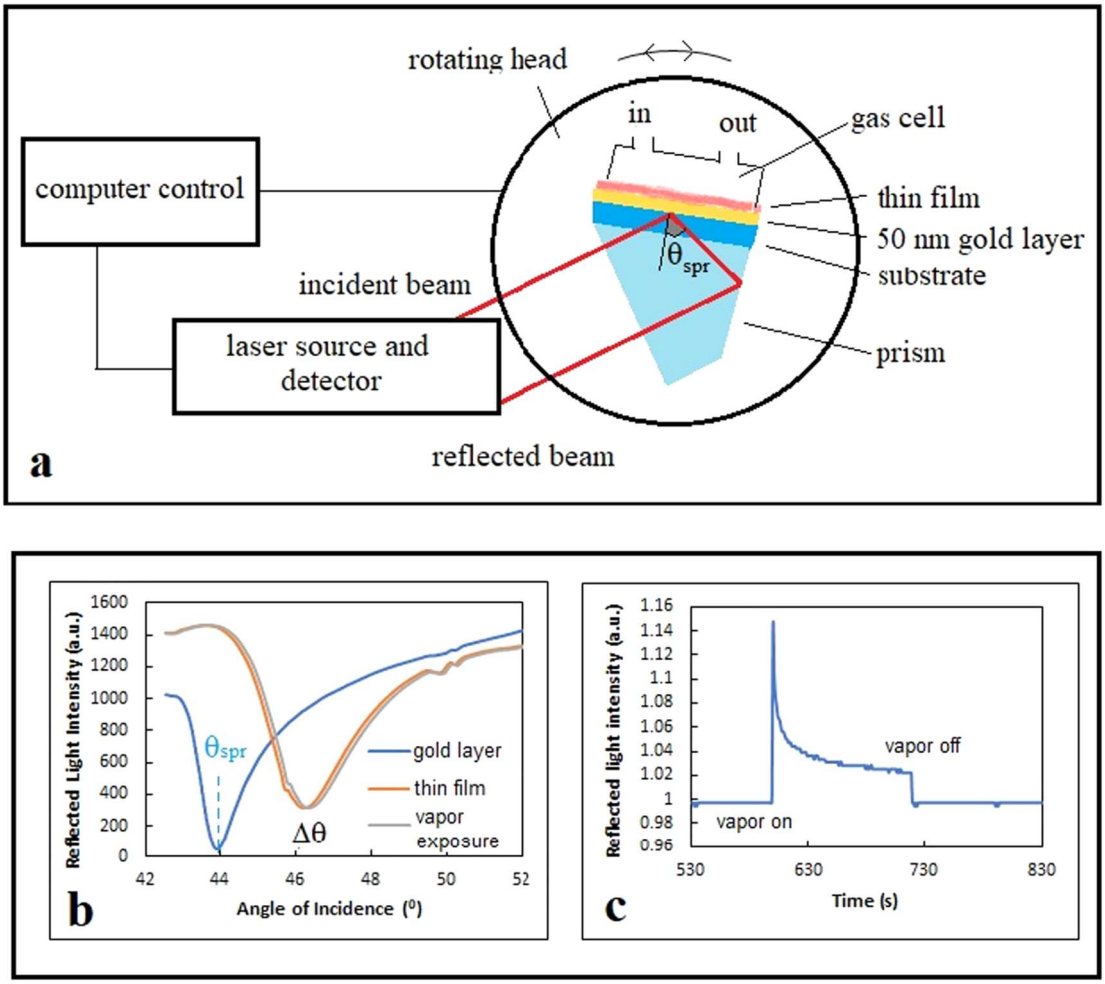

Figure 1. Schematic representation of the (a) SPR system, (b) SPR curve, and (c) kinetic measurement.

The solutions were prepared with the concentrations of 1 mg ml^{-1}, 2 mg ml^{-1} and 3 mg ml^{-1} using chloroform (supplied from Sigma Aldrich 99% and used without further purification) for each calixarene materials and used for the fabrication of the thin films.

2.2. Thin film fabrication

The spin coating technique was chosen for thin film fabrication to ensure the rapid formation of calix molecules on a solid surface. For this purpose, manually controlled Special Coating Systems (SCS) G3P-8 model spin coater was employed. A schematic representation of the spin coating instrument is presented in figure S1. 50 nm thick gold coated 20 × 20 × 1 mm glass slides (supplied from TEKNOTIP, Turkey) was cleaned with chloroform ultrasonically. The substrate was securely mounted onto the holder and maintained in place during spinning with the assistance of a vacuum pump. Rotation parameters were introduced to the spin coater via the control panel manually. Thin films of the calix molecules were fabricated in three steps immediately after the injection of 100 μl of the solution onto the substrate. In the first step the rotating table which was staying still starts to move so that spinning speed was increased up to 500 rpm in 11 s. During the second step spinning speed was increased to 1000 rpm in 25 s and kept constant at this spinning speed for another 10 s. Finally, the rotating table was stopped in 25 s from the spinning speed of 1000 rpm down to the stationary situation.

2.3. Vapor sensing properties of the spun thin films

BIOSUPLAR 6 Model 321 Surface Plasmon Resonance (SPR) system was employed to explore the vapor sensing properties of the calix thin films. The schematic illustration of the system is presented in figure 1(a). System consists of a rotating head which the thin film is attached onto, a laser source and a detector; all these components are computer controlled. The rotating head is composed of a glass prism with a refractive index of 1.517 which meets the He-Ne laser light of beam (632.8 nm) and projects the totally internal reflected light of

beam onto the detector with an angular resolution of 0.003°. The thin film deposited onto a 50 nm thick gold-coated glass substrate is attached onto one of the prisms' surfaces via index matching fluid with the same index of refraction as the glass prism. The gas cell is mounted onto the thin film surface which has inlet and outlet for the injected gas vapor. The movement of the rotating head provides the laser beam to be absorbed as result of the surface plasmon resonance at the special angle of incidence values (θ_{spr}) where because of the absorption of the laser beam, detected amount of the reflected light of intensity dramatically decreases. This phenomenon is observed via the SPR curves. Figure 1(b) presents the SPR curve for the uncoated gold substrate, the calix thin film coating, and the same thin film exposed to chlorinated VOC molecules.

The θ_{spr} depends on the optical constants of the prism and the metal film and expressed as [38]:

$$\theta_{SPR} = \sin^{-1}\left(\frac{\varepsilon_M}{\varepsilon_P(\varepsilon_M + 1)}\right)^{1/2} \quad (1)$$

where ε_P and ε_M denote the dielectric constant of the glass prism and metal film, respectively. The shift in the resonance angle resulting from the deposition of a thin layer on the metal surface and/or gas exposure to the thin film depends on the changes in film thickness, d, and the dielectric constant of the metal/thin film, as described by equation (2), and is expressed as follows [39]:

$$\Delta\theta_{SPR} = \frac{(2\pi/\lambda)(|\varepsilon_M|)^{3/2}d}{\sqrt{\varepsilon_P}\cos\theta(|\varepsilon_M - 1|)^2\varepsilon}(\varepsilon - 1) \quad (2)$$

where $|\varepsilon_M|$ represents the real component of the dielectric constant of the metal film coated on the gold surface, while ε denotes the dielectric constant of the thin film. The shift of the θ_{spr} in figure 1(b) with respect to gold substrates' θ_{spr} is directly related with the change in thickness and the optical constants.

The gas sensing properties of the thin films were analyzed using the kinetic measurements in which the time dependent amount of the reflected light intensity is monitored. A schematic representation of a kinetic measurement is presented in figure 1(c). Using the SPR curve of the thin film, an appropriate angle of incidence was selected and maintained during the kinetic measurements. The stable reflected light intensity was monitored for 120 s. Chlorinated VOCs were injected just after 120 s, resulting in a recorded change in reflected light intensity over another 120 s at the constant angle of incidence. This change was due to the interaction between the gas molecules and the thin film, which involved a diffusion phenomenon. At the end of this time interval, dry air was introduced into the gas cell to observe the recovery of the thin film. This experiment was repeated for each thin film using the saturated chloroform, dichloromethane and carbon tetrachloride vapors which were supplied from Sigma Aldrich with the purities of 99%. The kinetic measurements with the increasing concentration of the chlorinated VOCs were obtained by diluting the saturated vapor amount with the dry air in different volumes, therefore the 25%, 50%, 75%, and 100% saturated concentrations of each chlorinated VOCs were obtained. All measurements were carried through at the room temperature, with a relative humidity value of 25%. Our previous study on humidity effect of calixarene[4]arene thin using 36% RH and 76% RH values indicated that the humidity effect can be neglected [34].

2.4. Sensor parameters

The sensing characteristics are determined together with the sensor parameters of each interaction. Related parameters, which include response/recovery times, reproducibility, sensitivity, limit of detection and quantification were achieved via the real time kinetic graphs. Response time was described as the time needed to obtain the maximum response value after the injection of the vapor molecules. The recovery time was the time needed to reach the baseline response value after the injection of the dry air. The reproducibility was assessed by monitoring the response of the calixarene thin film sensors through reciprocal exposures to the analyte molecules within the gas cell. Consistent or preferably identical responses in terms of reflected light intensity indicated that a reproducible sensor had been successfully developed.

In this study, as stated before in the previous section, the volatile chlorinated vapor was injected into the gas cell in its saturated form and/or diluted portions of its saturated form. The concentration (c) values of the saturated vapor in ppm were calculated by equation (3) which is given by [11]:

$$c = \frac{22.4\rho V}{MV_0} \times 10^6 \quad (3)$$

where V_0 is the volume of the gas cell, V is the volume of injected vapor, ρ is the density of the selected vapor and M is the vapor molecular weight. The saturated concentration of the dichloromethane, chloroform and carbon tetrachloride vapors were calculated as 87.5×10^3 ppm, 69.9×10^3 ppm, and 57.8×10^3 ppm, respectively. This calculation is needed to obtain very important sensor parameters such as sensitivity (S), limit of detection (LOD) and limit of quantification (LOQ) parameters of a sensor. The sensitivity gives the quantity, how sensitive is a sensor material per unit concentration of vapor with the response in terms of reflected light

intensity rate. The kinetic response data was used to obtain the calibration curves. Using the slope of the linear relation between the response rate and the concentration, sensitivity of the sensor was calculated.

LOD and LOQ is related with the sensitivity presented in equations (4a) and (4b) [37, 40]:

$$LOD = \frac{3\sigma}{S} \tag{4a}$$

$$LOQ = \frac{10\,\sigma}{S} \tag{4b}$$

which indicates the minimum concentration of the vapor that can be detected and accurately quantified respectively where σ is the standart deviation of the sensing instrument used. All sensor parameters were obtained and will be presented in section 3.3.

2.5. Diffusion phenomena of the VOCs into thin films

Fick's second law of diffusion which offer a time dependent relation between the exposed and unexposed form of the thin film sensor in terms of the physical change. This law was applied to the experimental data to elucidate the diffusion process of the gas molecules. The kinetic data was recorded in 120 s of time intervals therefore data from the 120 s of the interaction interval during which the interaction between the thin film and chlorinated VOC molecules occurred was extracted from the kinetic measurements, normalized, and applied to equation (3). [41], where M_t and M_∞ represent the amount of vapor entering the thin film at any time t and the amount after saturation, respectively. Corresponding to these values, the reflected light intensities are denoted as $I_{rf}(t)$ and $I_{rf}(\infty)$, with D and a_o representing the diffusion coefficient and the initial thickness of the thin film at the beginning of the interaction, respectively. The normalized reflected light intensity decreases over time, indicating an inversely proportional relationship between the number of vapor molecules diffusing into the bulk of the thin film and the reflected light intensity, which can be expressed as shown in equation (5).

$$\frac{M_t}{M_\infty} \approx \left(\frac{I_{rf}(t)}{I_{rf}(\infty)}\right)^{-1} = 4\sqrt{\frac{D}{\pi a_0^2}}\,t^{\frac{1}{2}} \tag{5}$$

The linear relationship between the change in reflected light intensity and the square root of time was utilized to calculate the diffusion coefficients by applying the slope of the corresponding graph. The thickness of the thin films was estimated using WINSPALL software with an accuracy down to 0.001 nm, developed by the Wolfgang Knoll team at the Max Planck Institute for Polymer Research in Germany [42]. The software was used for the thickness and the optical constant determination in the literature [43].

3. Results and discussion

3.1. Thin film fabrication and characterization

Spin coated thin films of **CT2PA**, **C2PA**, and **CT4PA** calix materials were fabricated with a constant spinning speed of 1000 rpm. 100 μL of calix solution was injected onto the substrate for all fabrications. Solutions prepared with different concentrations (1 mg ml^{-1}, 2 mg ml^{-1}, and 3 mg ml^{-1}) were used to fabricate the thin films resulting with different thicknesses. The UV-Visible spectra of the spin-coated thin films fabricated from a 2 mg ml^{-1} solution are presented in figure S2. The formation of the thin layer is obvious in the UV-Visible spectra, similar formation of spun calixarene thin layers were presented in the literature [32]. The calixarene molecules have four aromatic phenyl rings, therefore they generally show strong absorption band at around 257–260 nm wavelength [44]. This is probably due to the π-π^* transition arising from the non-bonding electron in oxygen [45]. Each thin film of calix[4]arene derivatives was characterized by a single absorption peak at 280 nm, exhibiting a red shift of approximately 20 nm. This shift may result from molecular aggregation during the film formation on the solid substrate [46].

The alternative way to monitor the formation of the thin layers was SPR curve investigation. As described in section 2.3 the fabrication of the thin film onto 50 nm thick gold coated glass substrate results with a shift of the angle of incidence according to equation (2). In figure 2(a) the SPR curves for uncoated gold layer, spun thin films of calix materials using the solutions with the concentration of 2 mg ml^{-1} were presented. The gold layer has an SPR minimum (θ_{spr}) of 43.95° where this value was shifted to 47.08°, 46.71° and 46.34° for **CT2PA**, **C2PA**, and **CT4PA** thin films, respectively. The formation of a thin layer of the calix molecule is obvious for all materials. Different solutions prepared with the concentrations of 1 mg ml^{-1} and 3 mg ml^{-1} were used to fabricate the thin films with different thicknesses. The thin films prepared with the solution concentration of 1 mg ml^{-1} was expected to have a thinner film and the thin film prepared with the solution concentration of 3 mg ml^{-1} was expected as a thicker thin film with respect to the ones fabricated using 2 mg ml^{-1} of the solution concentration. In figure S3 the SPR curves of the **CT2PA**, **C2PA**, and **CT4PA** spun thin films were presented

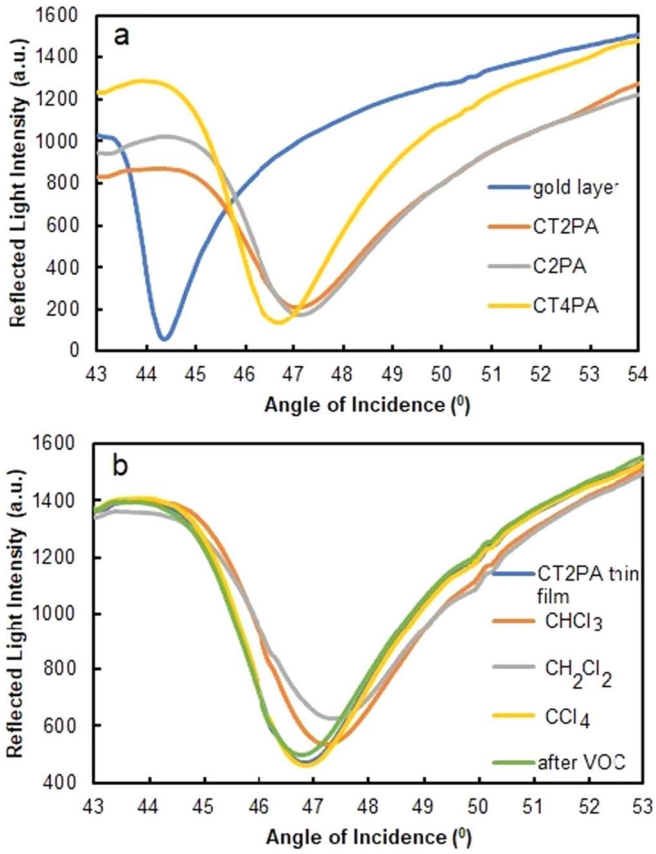

Figure 2. SPR curves of calix thin films (a) with the solution concentration of 2 mg ml^{-1} (b) **CT2PA** thin films fabricated with a solution concentration of 2 mg ml^{-1} during exposure to chloroform, dichloromethane and carbon tetrachloride vapors compared with the unexposed thin film and the SPR curves of the thin film after the exposure.

Table 1. The thickness, extinction coefficients and SPR angle minimum shift ($\Delta\theta$) values of the spun calix thin films fabricated with solutions of different concentrations.

Thin film	Solution concentration					
	1 mg ml^{-1}		2 mg ml^{-1}		3 mg ml^{-1}	
	$\Delta\theta$ (^{0})	d (nm)	$\Delta\theta$ (^{0})	d (nm)	$\Delta\theta$ (^{0})	d (nm)
CT2PA	1.91	8.59	3.13	10.32	2.82	11.92
C2PA	1.99	9.01	2.76	11.82	3.10	13.00
CT4PA	1.65	10.38	2.31	10.61	3.85	15.61

respectively for the increasing concentration of the solution. The shifts of the θ_{spr} were listed in table 1 with respect to the uncoated gold layer. The increasing demand with the increasing concentration was observed in all thin films except the **CT2PA** thin film fabricated with a solution concentration of 2 mg ml^{-1}.

By fitting the experimental SPR curve data to the equations (1) and (2), using the WINSPALL software, optical constants and the thickness of the calix thin films was estimated. The refractive index of the calix molecules was introduced as 1.5 and the extinction coefficient was equalized to zero referring to the previous studies [25, 47]. Thicknesses (d) of the thin films were fitted accordingly for all thin films under investigation and presented in table 1. An example of the fitting curve residing with the experimental SPR curve data of the **CT2PA** calix thin film fabricated using the solution concentration of 2 mg ml^{-1} is presented in figure S4. The estimated thickness values between 8.59 and 15.61 nm is in accordance with previous studies [32] with similar calixarene material. Additionally, the increase in thickness with the increasing concentration was observed for all calix materials as predicted.

The NT-MDT AFM NTEGRA Solaris model was utilized for atomic force microscopy (AFM) analysis. The instrument was operated in non-contact mode under ambient air conditions to investigate the surface properties of the films. The morphological characteristics of films on untreated, **CT2PA**-coated, **C2PA**-coated, and **CT4PA**-coated glass substrates were investigated using Atomic Force Microscopy (AFM) and Contact

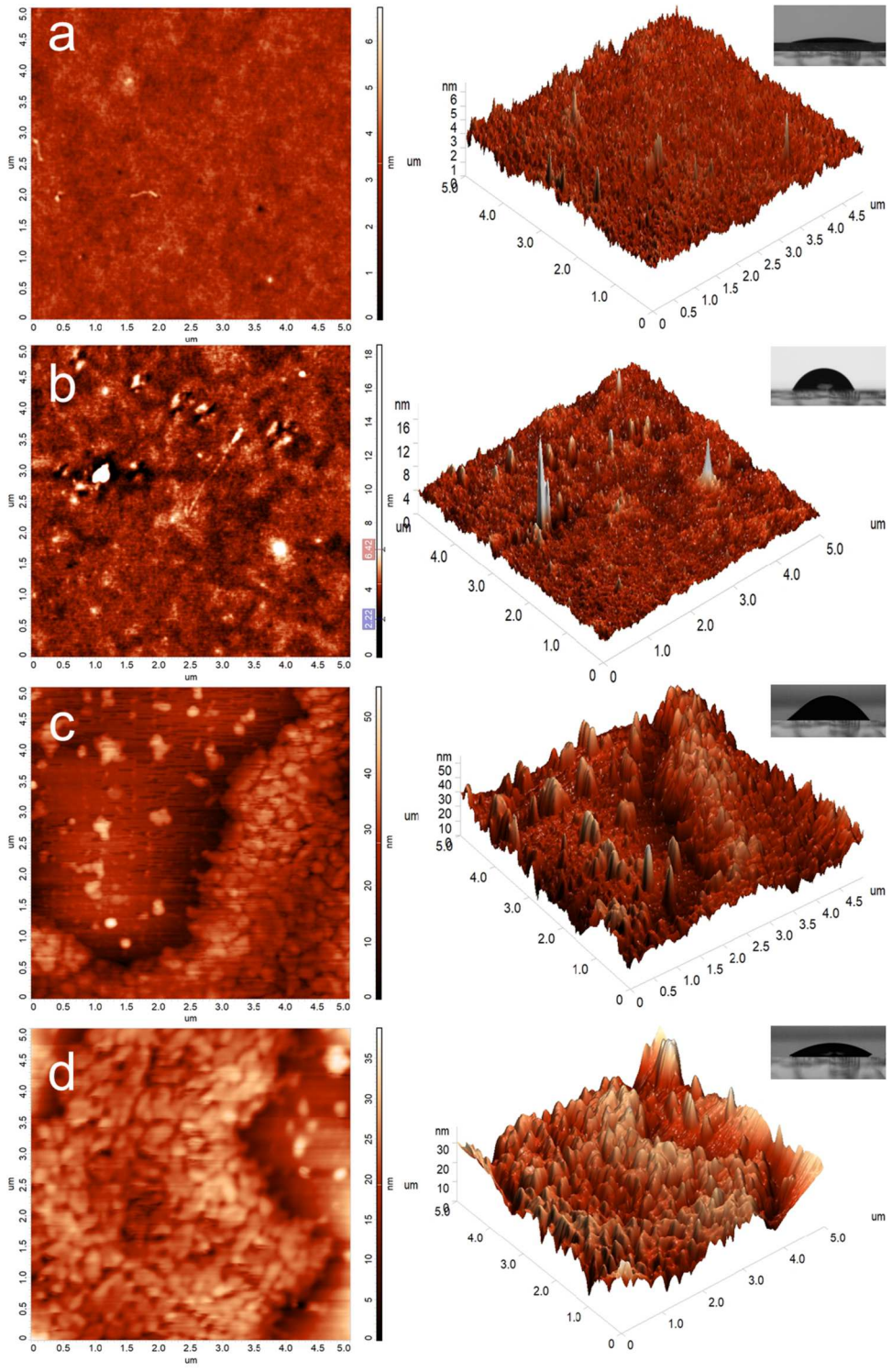

Figure 3. 2D and 3D AFM images and water contact angles of bare (a), **CT2PA** coated (b), **C2PA** coated (c), and **CT4PA** coated (d) glass surfaces.

Angle (CA) analysis. Figure 3 presents AFM images of the spin-coated thin films over a scanning area of $5 \times 5\,\mu m^2$, illustrating both 2D and 3D topographic representations of the calixarene derivative-coated substrates, which display a relatively uniform distribution across the glass surface. The AFM analysis reveals that the roughness values for the bare and coated glass surfaces are 0.2508 ± 0.09 nm, 0.4269 ± 0.11 nm, 5.0908 ± 0.26 nm, and 3.6855 ± 0.21 nm, respectively. Furthermore, the root mean square (rms) roughness values for these samples are 0.3268 ± 0.11 nm, 0.6804 ± 0.14 nm, 6.4868 ± 0.33 nm, and 4.6683 ± 0.25 nm, respectively. These findings may be attributed to the presence of phosphoric acid and tertiary butyl groups in the calixarene derivatives.

Table 2. Shift in the angle of incidence as a result of the exposure to saturated chlorinated vapor exposure.

	$\Delta\theta(^0)$				
	1 mg ml^{-1}	2 mg ml^{-1}			3 mg ml^{-1}
	CH_2Cl_2	$CHCl_3$	CH_2Cl_2	CCl_4	CH_2Cl_2
CT2PA	0.34	0.4	0.54	0.01	0.73
C2PA	0.15	0.13	0.14	0.02	0.10
CT4PA	0.36	0.5	0.54	0.13	0.99

Table 3. Physical properties of the analyzed chlorinated solvents.

	Vapor pressure at 25 °C (kPa)	Refractive index at 20 °C	Dipole moment (D)	Molar mass (g mol^{-1})
CH_2Cl_2	57.3	1.4244	1.6	84.93
$CHCl_3$	25.9	1.4459	1.15	119.37
CCl_4	11.94	1.4607	0	153.81

Contact angle measurements were conducted using the KSV CAM 200 instrument. Five consecutive measurements at different locations on the film surface were performed by assessing the contact angle of 5 μl sessile water droplets on the spun films. The average values obtained were employed for contact angle analysis. Insets of figure 3 display representative contact angle measurements for the spun film surfaces. The equilibrium contact angles for the bare, **CT2PA**-coated, **C2PA**-coated, and **CT4PA**-coated glass surfaces are measured at $6.12° \pm 0.57°$, $62.26° \pm 0.93°$, $47.55° \pm 1.07°$, and $26.83° \pm 1.21°$, respectively. It can be inferred that the water contact angle decreases with an increasing number of phosphoric acid groups present on the lower rim of the calixarene skeleton.

3.2. Responses of SPR curves with the injection of chlorinated VOCs vapors

The first observation of the gas sensing properties of the calix thin films was the alteration in the SPR curves during exposure to vapor molecules. The SPR curves for the **CT2PA** calix thin film, fabricated from a solution concentration of 2 mg mL^{-1}, are presented in figure 2(b) for the unexposed film, during exposure to saturated vapors of chloroform, dichloromethane, and carbon tetrachloride, and after flushing the gas cell with dry air. The SPR curves from the same experiment for the **C2PA** and **CT4PA** thin films are shown in figures S5(a) and (b), respectively. Following the injection of saturated chlorinated VOC vapors into the gas cell, a shift in the SPR curve to greater angles was observed, with recovery evident for all calix thin films after gas exposure. It is anticipated that the vapor molecules interact with the thin film in two steps: first through surface interaction, followed by diffusion into the bulk volume of the thin film. These two effects may alter the thickness and/or optical constants of the thin film, resulting in a shift in the resonance angle as described by equation (2).

The highest shift observed during the interaction of the thin films with the CH_2Cl_2 vapor was remarkable so, the interaction of the CH_2Cl_2 vapor was deeply investigated for the calix thin films fabricated with the solutions of different concentrations. The shifts in the SPR minimum were listed in table 2 for all calix thin films under investigation. The maximum shifts among the chlorinated VOCs vapors were observed for CH_2Cl_2 vapor for the thin films fabricated with a solution concentration of 2 mg ml^{-1}. Amount of the shift in the SPR angle was in the order of **CT4PA** > **CT2PA** > **C2PA** substantially for the three chlorinated vapors.

The minimum interaction magnitude among the chlorinated vapors were carbon tetrachloride. This phenomenon can be explained via the physical properties of the vapors presented in table 3. It is well established that a higher dipole moment of the vapor enhances the interaction between the gas vapor molecules and the thin film molecules through reversible dipole–dipole interactions [48, 49]. Carbon tetrachloride vapor that has no dipole moment was not able to incorporate into this kind of interaction. Chloroform and dichloromethane vapors both having net dipole moments were holding this physical advantage during the interaction process.

Higher vapor pressure of the vapors may be another important physical property that affects the sensing properties [10]. The lowest vapor pressure of the carbon tetrachloride vapor between all vapors examined is also obvious in table 3 that can also be another concluding remark to explain its low interaction with the calixarene thin films.

The interaction of vapor molecules with the calixarene thin films is characterized by a diffusion mechanism that begins with surface interactions, followed by subsequent diffusion into the bulk of the thin film [8]. The porous structure of the calixarene layers allows the diffusion of the vapor molecules into the thin film matrix even with low concentrations. This yields a low volume, thus a low mass of a vapor molecule to diffuse into the bulk structure of the thin film. Bigger molar mass of the molecule may reduce the diffusion of the gas molecules into the bulk of the thin film which can clarify the very low interaction of CCl_4 vapor molecules within the thin film [44]. The shift of the SPR curve during the gas interaction is a result of the change in the optical constants therefore, the gap between the vapor molecules' and the thin films' refractive indexes (Δn) may be effective on the SPR curve shift [50, 51]. The refractive index of the calix thin films was 1.5 so, the biggest gap between the thin film and the vapor molecules was existing in the order of $CH_2Cl_2 > CHCl_3 > CCl_4$ which is similar with the interaction magnitude order. Similar results were also revealed in the literature in the previous studies [11, 44].

The interaction of the CH_2Cl_2 vapor with the thin film was deeply investigated because of thin films' highest response to CH_2Cl_2. The concentration dependence was studied by the fabrication of the thin films with the solution concentrations of 1 mg ml^{-1} and 3 mg ml^{-1} in addition to the thin film fabricated using the solution concentration of 2 mg ml^{-1}. The response values in terms of the SPR minimum shift ($\Delta\theta$) was increasing with the increasing solution concentration for **CT2PA** and **CT4PA** thin films; correlatively increasing with the thickness. The effect of the thickness of the layers on the response was shown in the literature [52] which concentrate on the thickness dependence of the mixed porphyrin and calixarene thin films' response. Thicker the thin film facilitates the interaction of the gas molecules with the bulk volume of the thin film through diffusion, which will be explained in the oncoming sections. The response for the **C2PA** thin film was the opposite of this behavior, which may be related with its molecular structure.

3.3. Kinetic responses of calix films and sensor parameters

Time dependent responses in terms of the reflected light intensity change ΔI (a.u.) during the exposure to vapor molecules were presented in figure 4. The kinetic response of the thin films fabricated using the solution concentration of 2 mg ml^{-1} were used to investigate the response towards the increasing concentrations of the chlorinated solvent vapors. All thin films determine an increasing demand in the reflected light intensity accompanied by the increasing vapor concentration. Four reciprocal exposures of the saturated vapor concentrations under investigation were presented with the inset of the figures. The inset possesses a similar response in each cycle supporting the reproducibility of the calixarene thin sensor layers. At the end of each cycle as a result of dry air injection, the reflected light intensity is recovered to the initial value. This allows the ending of the host–guest interaction which is reversible in nature, therefore, the stability of the interaction is obtained. Similar results were observed in previous work [53]. The highest magnitude of the response was observed for the **CT4PA** thin film during exposure of each chlorinated volatile vapors. The smallest response was observed for the **C2PA** thin film. The different adsorption behavior of volatile organic compounds may be attributed to the both different symmetry and polarity of chlorinated vapors, and presence of polar phosphonic acid units of calix[4]arene skeleton. But the relative amounts of adsorption response towards volatile organic compounds are also influenced by number of phosphonic acid groups onto the lower rim of calix[4]arene skeleton. Because, a large number of electron donor phosphonic acid units on the surface of thin film increase the dipole–dipole and hydrogen bonding interactions between calixarene skeleton and organic vapors [54]. Comparing the numbers of phosphonic acid units available on the lower rim of calixarene skeleton (phenolic hydroxy groups), **CT4PA** having four phosphonic acid units have shown excellent binding response towards dichloromethane vapor which has high dipole moment value (1.60D) with respect to the other chlorinated vapors, chloroform (1.04D) and carbon tetrachloride (0D) [32]. Furthermore, it is possible that the interaction between the chlorine atom of dichloromethane and the lone pair electrons of the phosphonic acid groups in **CT4PA** facilitates the preorganization of the macromolecule through optimal dipole–dipole interactions. Additionally, although all the calixarene derivatives share the same chemical structure, **CT2PA** and **C2PA**, which contain two phosphonic acid units at their 1,3-distal positions [55, 56], do not provide suitable dipole–dipole binding sites for the other VOC molecules compared to **CT4PA**.

Similar effect was observed for the thin films fabricated using different solution concentrations (1 mg ml^{-1} and 3 mg ml^{-1}). Kinetic graphs were given in figure S6 for the **CT2PA**, **C2PA**, and **CT4PA** thin films fabricated via solutions with different concentrations. The increasing response with the increasing concentration was observed for all thin films where the least response was observed for the **C2PA** thin film.

Kinetic interaction between the vapor molecule and the calixarene thin film was carried on for 2 min for each experiment. The interaction interval of a few seconds was obtained for all calixarene-vapor interaction. A longer period of time—10 min was let the calixarene thin film to observe any difference which may occur in the interaction characteristics. The kinetic graph was presented in figure S7 showing the long term kinetic

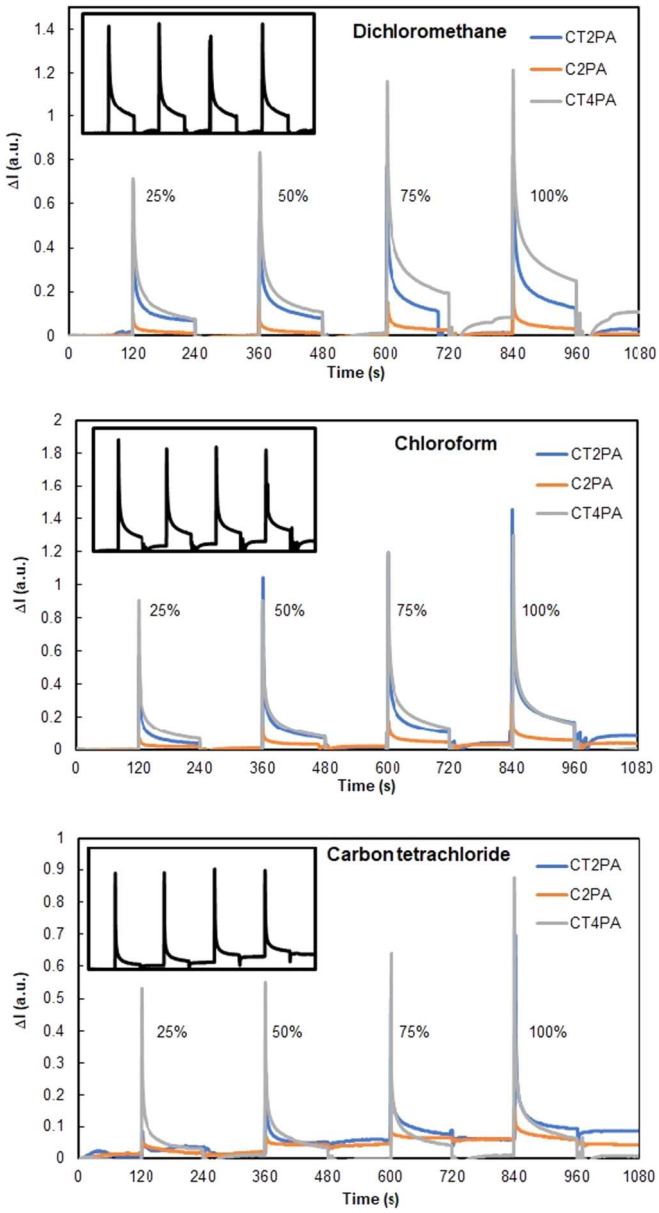

Figure 4. Kinetic graphs of the **CT2PA**, **C2PA**, and **CT4PA** thin films fabricated with the solution concentration of 2 mg ml^{-1} during the exposures chlorinated vapors with increasing saturated concentrations. Inset in the figures are the kinetic graphs for the reciprocal exposure of the **CT2PA** thin films to the analyte vapor under examination.

interaction. It is observed that the kinetic characteristics was not changing with time. The period of 120 s was sufficient to observe the calix thin film - vapor interaction.

The quantification of the sensor response is important for a deep investigation of a calixarene sensor. Therefore, the sensor parameters such as response/recovery times, sensitivity and LOD/LOQ values of each calixarene thin film sensors were studied. The response times obtained using the kinetic graphs were between 1–2 s and the recovery times were between 2–4 s for all calixarene thin film sensors. The time interval was not dependent on the calixarene type (**CT2PA**, **C2PA**, **CT4PA**) and was not affected with any of the chlorinated vapor type under examination. The previous gas sensing studies on the calixarene layers in the literature were reviewed and similar response and recovery times were confirmed. The response and recovery range in just a few seconds were reached for the dichloromethane vapor as distinct from the other volatile vapor toluene and explosive vapor DNT [12]. Another study involving calix[4], calix[6] and calix[8] also revealed the response and recovery times of only a few seconds through volatile organic vapors such as chloroform, benzene, toluene and ethanol [53].

Following sensor parameters; sensitivity, LOD and LOQ were determined with the help of the calibration curves presented in figure 5. The calibration curves of the calixarene thin films fabricated using the solution concentration of 2 mg ml^{-1} were given for each chlorinated vapor. They exhibit an increasing response rate

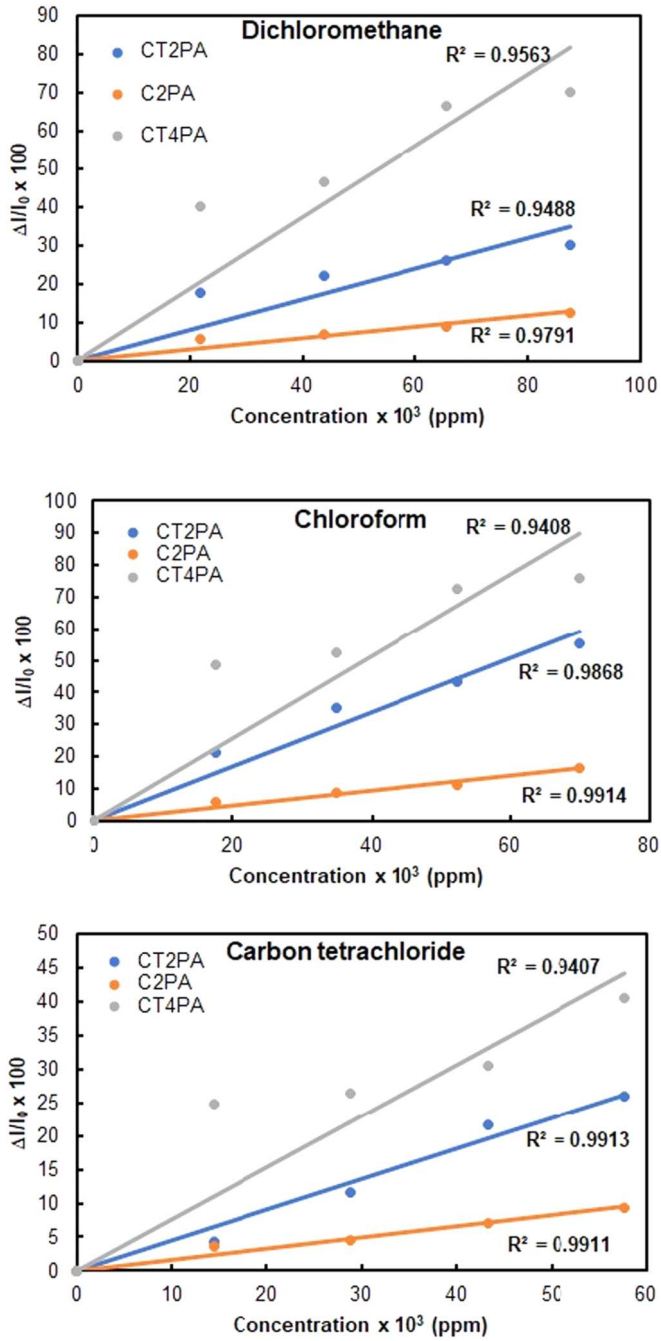

Figure 5. Calibration curves for the kinetic measurements for each chlorinated vapor.

with the increasing concentration, with the regression coefficients (R^2) near to unity is the evidence of the linear relation. The calibration curves for the thin films fabricated using different solution concentrations of the calixarene molecules were presented in figure S6. Similar behavior was observed for this calixarene thin film sensors; the regression coefficients were close to unity and the linear dependence of the response rate with the vapor concentration was obvious as expected. The slopes of the linear lines; sensitivities (S) were presented in table 4 in terms of the response rate per concentration in ppm of the related chlorinated vapor for all thin films under investigation. Accordingly, the LOD and LOQ values of the calixarene thin films were calculated using the equations (4a) and (4b) and presented in table 4. Among the chlorinated vapors under examination the maximum sensitivity values were obtained for the chloroform vapor. This behavior is accompanied by the minimum value of LOD and LOQ values for the thin films fabricated under the same conditions. A dependence of the solution concentration on the response was not observed.

Previous work on the VOCs sensing properties of the calixarene thin layers and reported sensor parameters are listed in table 5. The LOD values in the SPR study with LB thin films of the pyridine modified calixarene thin films were much higher than this work [57]. Additionally, spun phosphonated calixarene bearing crown ether

Table 4. Sensitivity, LOD and LOQ values of the calixarene thin film sensors.

Analyte vapor		CH_2Cl_2 1 $mgml^{-1}$	$CHCl_3$	CH_2Cl_2 2 $mgml^{-1}$	CCl_4	CH_2Cl_2 3 $mgml^{-1}$
CT2PA	**S** $\times$ **10**$^{-3}$**(ppm**$^{-1}$**)**	0.84	0.85	0.39	0.45	0.56
	LOD (ppm)	4	4	8	7	5
	LOQ (ppm)	12	12	25	22	18
C2PA	**S** $\times$ **10**$^{-3}$**(ppm**$^{-1}$**)**	0.18	0.23	0.14	0.16	0.14
	LOD (ppm)	16	13	21	18	21
	LOQ (ppm)	55	40	69	61	71
CT4PA	**S** $\times$ **10**$^{-3}$**(ppm**$^{-1}$**)**	1.03	1.29	0.93	0.77	1.43
	LOD (ppm)	3	2	3	4	2
	LOQ (ppm)	10	8	11	13	7

Table 5. Comparison with the previous work.

Method	Studied analyte vapors	Sensitivity	LOD (ppm)	Response time	References
	Dichloromethane	Hz ppm^{-1}			
	Chloroform	2.023			
QCM	Benzene	(Only for dichloromethane)	1.482	Not reported	[54]
	Toluene				
		Intensity shift ppm^{-1}	$\times 10^3$		
	Acetone	0.477	7.79		
SPR	Chloroform	0.394	7.48		
	Methanol	0.097	14.50	3 s	[57]
	Ethyl acetate	0.214	6.07		
	Benzene	0.185	6.52		
		Response ppm^{-1}	$\times 10^3$		
	Chloroform	0.47×10^{-3}	10.23		
SPR	Carbon tetrachloride	0.33×10^{-3}	5.07		
	Dichloromethane	0.298×10^{-3}	17.01	Not reported	[32]
	Ethanol	0.12×10^{-3}	39.02		
	Benzene	0.082×10^{-3}	23.0		
	Toluene	0.028×10^{-3}	25.02		
		Response rate ppm^{-1}			
	Chloroform	0.152×10^{-3}	21.71		
SPR	Dichloromethane	0.115×10^{-3}	28.69		
	Carbon tetrachloride	0.078×10^{-3}	42.31	1–3 s	[11]
	Trichloroethylene	0.036×10^{-3} ppm^{-1}	91.66		
	Dichloromethane	8.55×10^{-4}	3.51		
SPR	Chloroform	9×10^{-4}	3.33	Not reported	[37]
	Benzene	15.8×10^{-4}	1.89		
	Toluene	17.29×10^{-4}	1.74		

thin films also shown much higher LOD values compared with this work [32]. Spun thin films of sulfonated calixarene molecules shown better LOD values [11] where the best LOD values in the literature was obtained with the LB thin films of phosphonated calixarene molecules [37]. In addition to this, reported response times are in accordance with this work. Among several group of VOCs listed, chlorinated compounds feature heavily in higher sensitivity levels with lower limit of detection values. Therefore, we preferred to focus on the chlorinated vapor sensing in this work.

3.4. Density functional theory calculation

To better understand the nature of the complexation capability of **CT4PA** with volatile organic compounds (CCl_4, CH_2Cl_2, and $CHCl_3$), geometric optimizations and theoretical calculations of **CT4PA** and its inclusion complexes were verified by applying density functional theory (DFT) with B3LYP and 6-311G (d, p) basis. DFT calculations were conceded using Gaussian 09 program [58]. The optimized geometries of **CT4PA** and its inclusion complexation forms are given in figure 6. In the complex, VOC compounds generally prefer to coordinate with phosphonic acid units of **CT4PA** by dipole–dipole interaction mechanism. LUMO and HOMO dispersions and energies of complex structure of **CT4PA** were calculated. As shown in figure 6., the

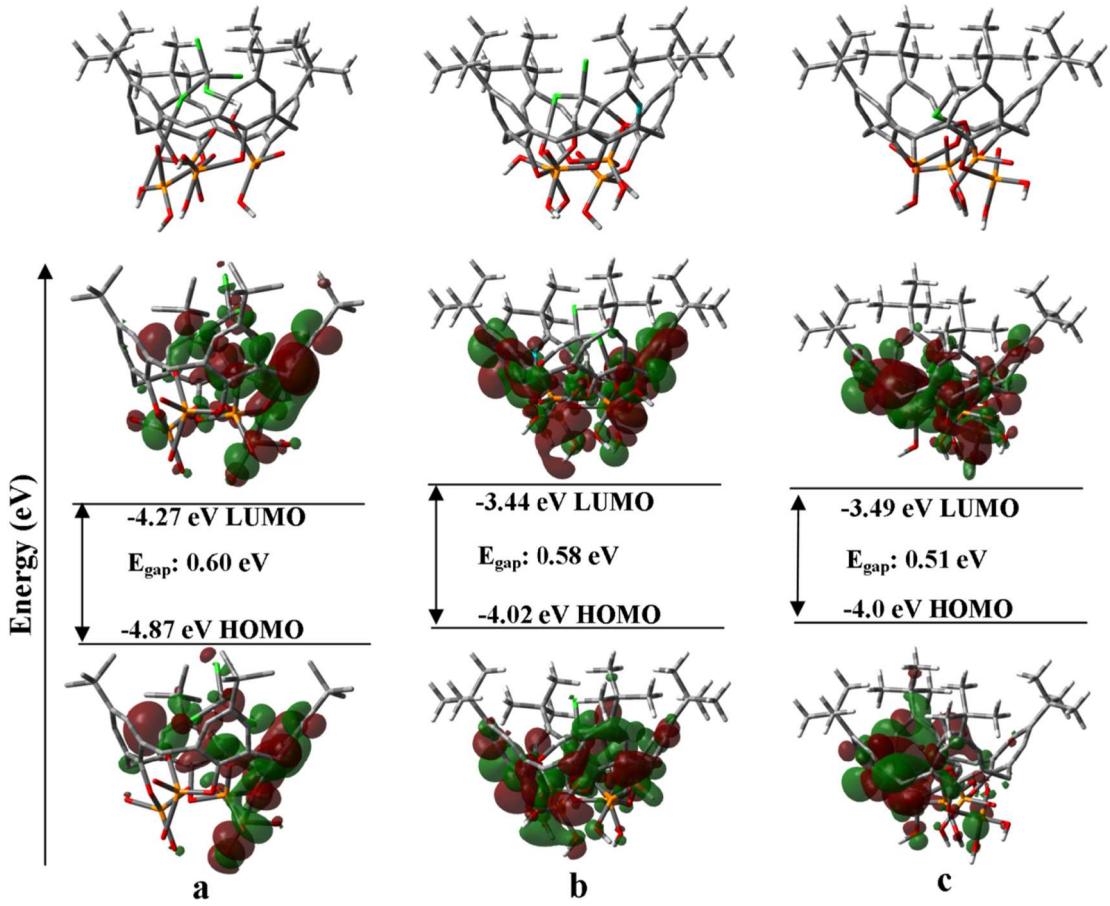

Figure 6. Optimize structures and energy diagrams of HOMO and LUMO orbitals; (a) **CT4PA-CCl_4**, (b) **CT4PA-CH_2Cl_2**, and (c) **CT4PA-$CHCl_3$** inclusion complexes.

LUMO and HOMO orbitals are located in different parts of **CT4PA** complexes. In the case of inclusion complexation forms of **CT4PA**, HOMO orbital is primarily dispersed on the two phenyl rings and two methylene bridges of calixarene skeleton [59] for both chloroform and dichloromethane whereas same orbital is distributed on both phenyl rings and two phosphonic acid groups of **CT4PA** for carbon tetrachloride. Compared the HOMO and LUMO orbitals, LUMO orbitals are commonly located both onto the entire molecule (**CT4PA**) and two phosphate groups of calixarene skeleton in the face of the guest molecule. The energy gaps between the LUMO and HOMO of **CT4PA** inclusion complexes were 0.60 eV for CCl_4, and 0.58 eV for CH_2Cl_2 complexes, whereas the energy gaps for **CT4PA-$CHCl_3$** were found to be 0.51 eV, respectively. These calculations indicated that LUMO–HOMO energy gaps of complexes slightly reduced with increasing dipole moment values and stabilized the system owing to the possible interaction between **CT4PA** and $CHCl_3$ [60]. Therefore, theoretical data are in agreement with the obtained sensor results.

3.5. Diffusion phenomena of chlorinated VOCs into calix thin films

The evaluation of the interaction between VOC molecules and the **CT2PA**, **C2PA**, and **CT4PA** thin films—specifically the adsorption process within the bulk structure of the thin film—warrants thorough investigation. Ficks' Law of diffusion was used to investigate this behavior in which the molar flux is integrated with the concentration gradient which is proportional with the diffusion [24]. This model can be used to explain the VOCs diffusion into the bulk of the thin films. The kinetic data in figures 4 and S6 was picked over for the 120 s of the time period in which the VOCs molecules were injected into the gas cell. Normalized data was presented in figure S9 for the saturated chloroform vapor exposure to CT4PA thin film. This transaction was applied to all data and obtained graph has been converted into the dependence between the $I_{rf}(\infty)/I_{rf}(t)$ and $t^{1/2}$ through the linear relationship via equation (5) in order to calculate the diffusion constant. The obtained graph was presented in figure S9. The linear dependence was anticipated according to the equation where the two linear regions in each graph were remarkable. First linear region was approximately lasting through the first 10 s of the diffusion process. This first region 'adsorption' offers a fast interaction between the vapor and the calixarene thin film with a steep slope. The interaction between the time interval of 11 s to 120 s was the second region of

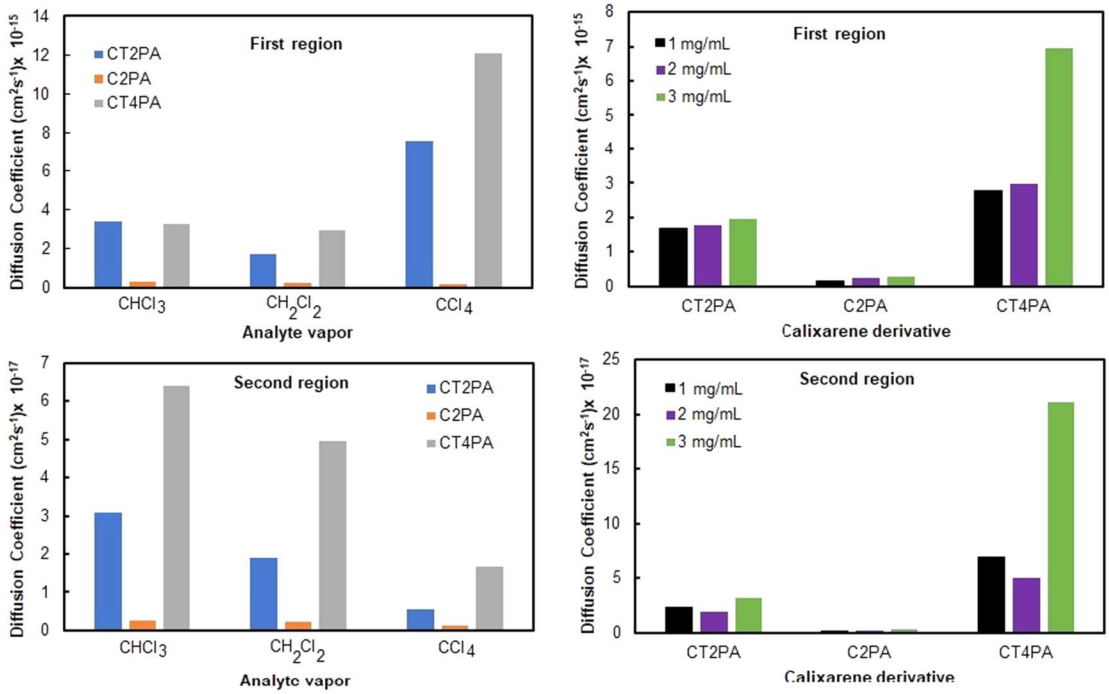

Figure 7. Diffusion coefficients of the chlorinated hydrocarbon vapors in the first and second region of the interaction.

the diffusion. This region gives the clue of a much slow penetration probably through the inner bulk structure of the calixarene thin film. This kind of interaction was proposed in the literature for the calixarene layers [25] evaluating the vapor molecule size to penetrate into the thin film structure by the diffusion process. The adsorption/diffusion phenomenon of the several volatile organic compounds was also shown for calixarene materials fabricated via Langmuir Blodgett thin film fabrication technique [10].

The slopes of the two interaction regions were different from each other, thus providing different diffusion coefficients; the first and the second region were presented in figure 7 for all of the chlorinated hydrocarbon vapor interactions through the calixarene thin films fabricated with a solution concentration of 2 mg ml^{-1}. The values of the diffusion coefficients and all regression coefficients can also be found in table S1 in detail.

The fast interaction of the carbon tetrachloride in the first region (surface interaction) was observed with higher diffusion coefficient values. In the case of the penetration into the bulk of the structure through the second region, the dominating character of the chloroform vapor mobility was observed via the highest diffusion coefficients for the chloroform vapor. This behavior also corroborates the results presented in section 3.2. The higher dipole moments and vapor pressures together with the lower molar mass and refractive index values of the chloroform and dichloromethane vapors were presented to easily interact with the calixarene thin films. The higher interaction of the **CT4PA** calix molecule with the vapors were also observed via the highest diffusion coefficients for the **CT4PA** thin films. The previous result on the order of the interaction magnitude **CT4PA** > **CT2PA** > **C2PA** was supported once again with the diffusion coefficients.

The kinetic response graphs studied for the dichloromethane interaction of the calixarene thin films fabricated with different solution concentration values were also analyzed to calculate the diffusion coefficients. The results were presented in figure 7 and the diffusion coefficients and all regression coefficients were given in table S2. It is observed that increasing the solution concentration was leading to a slight increase in the diffusion coefficient. High solution concentration, therefore thicker thin film was found to be highly interacting with the vapor molecule which was previously proposed in section 3.2. The highest diffusion coefficients were calculated for the **CT4PA** thin films which is again in accordance with the evaluations in the previous sections.

4. Conclusion

Phosphonate based lipophilic calix[4]arene thin films for the chlorinated vapor sensing were found to be a good alternative as candidate for gas detecting with an affinity to detect chloroform and dichloromethane vapor molecules compared with the carbon tetrachloride. This behavior was evaluated via the physical properties of the vapor molecules. The high dipole moment and vapor pressure together with the low molar mass and

refractive index of the analyte vapor molecules were found to be effective on the high sensitivity. Sensor parameters for these developed sensors possess low response and recovery times down to a few seconds and high sensitivity up to 1.29×10^{-3} ppm^{-1} and a good reproducibility. The chemical structure of the calix[4] arene molecules with different number of phosphonic acid groups were taken into consideration upon the possible interaction mechanisms of the functional groups. The time dependent gas sensing kinetics was modeled using Ficks' law of diffusion which fits the experimental data by a two-region interaction model. In addition, the theoretical calculation between chlorinated volatile organic compounds and calixarene molecule was also studied and it was found that the energy gap between calixarene molecule and chloroform vapor was lower compared to other volatile compounds. It can be concluded that the **CT4PA** thin film sensor is a good nominee for the chlorinated volatile organic vapor sensing.

Acknowledgments

The authors wish to express their gratitude to the EngSurf-Twin project, which is funded by the EU Horizon 2020 program (Grant Number 952289).

Data availability statement

All data that support the findings of this study are included within the article (and any supplementary files).

References

[1] Lei C, Liang F, Li J, Chen W and Huang B 2019 Electrochemical reductive dechlorination of chlorinated volatile organic compounds (Cl-VOCs): effects of molecular structure on the dehalogenation reactivity and mechanisms *Chem. Eng. J.* **358** 1054–64
[2] Bale A S, Barone S, Scott C S and Cooper G S 2011 A review of potential neurotoxic mechanisms among three chlorinated organic solvents *Toxicol. Appl. Pharmacol.* **255** 113–26
[3] Halios C H, Landeg-Cox C, Lowther S D, Middleton A, Marczylo T and Dimitroulopoulou S 2022 Chemicals in European residences —Part I: a review of emissions, concentrations and health effects of volatile organic compounds (VOCs) *Sci. Total Environ.* **839** 156201
[4] Mangotra A and Singh S K 2024 Volatile organic compounds: A threat to the environment and health hazards to living organisms—a review *J. Biotechnol.* **382** 51–69
[5] Huang B, Lei C, Wei C and Zeng G 2014 Chlorinated volatile organic compounds (Cl-VOCs) in environment — sources, potential human health impacts, and current remediation technologies *Environ. Int.* **71** 118–38
[6] Pinalli R, Pedrini A and Dalcanale E 2018 Environmental gas sensing with cavitands *Chemistry—A European Journal* **24** 1010–9
[7] Vinodh M, Alipour F H, Mohamod A A and Al-Azemi T F 2012 Molecular assemblies of porphyrins and macrocyclic receptors: Recent developments in their synthesis and applications *Molecules* **17** 11763–99
[8] Kumar S, Chawla S and Zou M C 2017 Calixarenes based materials for gas sensing applications: a review *J. Inclusion Phenom. Macrocyclic Chem.* **88** 129–58
[9] Sundramoorthy A K *et al* 2015 Lateral assembly of oxidized graphene flakes into large-scale transparent conductive thin films with a three-dimensional surfactant 4-sulfocalix[4]arene *Sci. Rep.* **5** 10716
[10] Şen S, Davis F, Çapan R, Özbek Z, Özel M E and Stanciu G A 2020 A macrocyclic tetra-undecyl calix[4]resorcinarene thin film receptor for chemical vapour sensor applications *J. Inclusion Phenom.Macrocyclic Chem.* **98** 237–47
[11] Çapan R, Çapan İ, Davis F and Ray A K 2024 Spin-coated films of calix[4]resorcinarenes as sensors for chlorinated solvent vapours *J. Mater. Sci., Mater. Electron.* **35** 1701
[12] Montmeat P, Veignal F, Methivier C, Pradier C M and Hairault L 2014 Study of calixarenes thin films as chemical sensors for the detection of explosives *Appl. Surf. Sci.* **292** 137–41
[13] Tisserant J-N, Beck S, Barf M-M, Kowalsky W and Lovrincic R 2018 Nanoporous organic field-effect transistors employing a calixarene dielectric for sub-ppb gas sensing *Adv. Electron. Mater.* **4** 1800362
[14] El Kazzy M *et al* 2021 An overview of artificial olfaction systems with a focus on surface plasmon resonance for the analysis of volatile organic compounds *Biosensors* **11** 244
[15] Chiu N-F 2022 The current status and future promise of SPR biosensors *Biosensors* **12** 933
[16] Kumar V, Raghuwanshi S K and Kumar S 2022 Recent advances in carbon nanomaterials based SPR sensor for biomolecules and gas detection—a review *IEEE Sens. J.* **22** 15661–72
[17] Singh P 2016 SPR biosensors: Historical perspectives and current challenges *Sensors Actuators B* **229** 110–30
[18] Chen T, Xin J, Chang S J, Chen C-J and Liu J-T 2023 Surface plasmon resonance (SPR) combined technology: A powerful tool for investigating interface phenomena *Adv. Mater. Interfaces* **10** 2202202
[19] Lakkis S, Younes R, Alayli Y and Sawan M 2014 Review of recent trends in gas sensing technologies and their miniaturization potential *Sensor Rev.* **34** 24–35
[20] Köβlinger C *et al* 1995 Comparison of the QCM and the SPR method for surface studies and immunological applications *Sensors Actuators B* **24** 107–12
[21] Kim J, Kim S, Ohashi T, Muramatsu H, Chang S-M and Kim W-S 2010 Construction of simultaneous SPR and QCM sensing platform *Bioprocess. Biosyst. Eng.* **33** 39–45
[22] Mivehi L, Bordes R and Holmberg K 2013 Adsorption of cationic gemini surfactants at solid surfaces studied by QCM-D and SPR—Effect of the presence of hydroxyl groups in the spacer *Colloids Surf., A* **419** 21–7
[23] Yesudasu V, Pradhan H S and Pandya R J 2021 Recent progress in surface plasmon resonance based sensors: a comprehensive review *Heliyon* **7** e06321

[24] Davis F, Higson S P J, Oliveira O N Jr and Shimizu F M 2020 Calixarene-based gas sensors ed S Thomas *et al Functional Nanomaterials: Advances in Gas Sensing Technologies* (Springer) 433–62
[25] Kostyukevych K V *et al* 2016 A nanostructural model of ethanol adsorption in thin calixarene films *Sensors Actuators B* **223** 470–80
[26] Kostyukevych K V, Khristosenko R V, Shirshov Y M, Kostyukevych S A, Samoylov A V and Kalchenko V I 2011 Multi-element gas sensor based on surface plasmon resonance: recognition of alcohols by using calixarene films *Semiconductor Physics, Quantum Electronics & Optoelectronics* **14** 313–20
[27] Halay E, Bozkurt S, Capan R, Erdogan M, Unal R and Acikbas Y 2020 Calix[4]arene-triazine conjugate intermediate: optical properties and gas sensing responses against aromatic hydrocarbons in Langmuir–Blodgett films *Res. Chem. Intermed.* **46** 4433–45
[28] Hassan A K, Ray A K, Nabok A V and Wilkop T 2001 Kinetic studies of BTEX vapour adsorption onto surfaces of calix-4-resorcinarene films *Appl. Surf. Sci.* **182** 49–54
[29] Ozkaya C, Capan R, Erdogan M, Bayrakci M, Ozmen M and Acikbas Y 2020 Fabrication of picoline amide-based calix[4]arene Langmuir-blodgett thin film for volatile organic vapor sensing application *Mol. Cryst. Liq. Cryst.* **710** 49–65
[30] Çapan R *et al* 2010 Characterization of langmuir–blodgett films of a calix[8]arene and sensing properties towards volatile organic vapors *Sensors Actuators B* **148** 358–65
[31] Özbek Z *et al* 2011 Optical parameters of calix[4]arene films and their response to volatile organic vapors *Sensors Actuators B* **158** 235–40
[32] Capan I, Bayrakci M, Erdogan M and Ozmen M 2019 Fabrication of thin films of phosphonated calix[4]arene bearing crown ether and their gas sensing properties *IEEE Sens. J.* **19** 838–45
[33] Cheng T, Li J, Ma X, Zhou L, Wu H and Yang L 2023 Behavior of VOCs competitive adsorption with water vapor in a slit-shaped phosphoric acid mesoporous activated carbon model *Sep. Purif. Technol.* **326** 124776
[34] Çapan R, Çapan İ and Davis F 2023 A new approach for the adsorption kinetics using surface plasmon resonance results *Sensors Actuators B* **394** 134463
[35] Erdoğan M, Çapan R and Davis F 2010 Swelling behaviour of calixarene film exposed to various organic vapours by surface plasmon resonance technique *Sensors Actuators B* **145** 66–70
[36] Ozcelik E, Tabakci B, Karaman M and Tabakci M 2025 Calixarene-based functional fabric for simultaneously adsorptive removal of anionic and cationic dyes *ACS Omega* **10** 181–92
[37] Capan I, Capan R, Erdogan M, Bayrakci M and Ozmen M 2022 Sensing behaviors of lipophilic calix[4]arene phosphonate based Langmuir-Blodgett thin films for detection of volatile organic vapors *Sens. Actuators, A* **347** 113947
[38] Knoll W 1998 Interfaces and thin films as seen by bound electromagnetic waves *Annu. Rev. Phys. Chem.* **49** 569–638
[39] Pockrand I 1978 Surface plasma oscillations at silver surfaces with thin transparent and absorbing coatings *Surf. Sci.* **72** 577–88
[40] Gauglitz G 2018 Analytical evaluation of sensor measurements *Anal. Bioanal.Chem.* **410** 5–13
[41] Erdoğan M, Çapan İ, Tarimci Ç and Hassan A K 2008 Modeling of vapor sorption in polymeric film studied by surface plasmon resonance spectroscopy *J. Colloid Interface Sci.* **323** 235–41
[42] Ji L, Chen Y and Yuan Y J 2014 Investigation of surface plasmon resonance phenomena by finite element analysis and Fresnel calculation *Sensors Actuators B* **198** 82–6
[43] Şen S, Çapan R, Özbek Z, Özel M E, Stanciu G A and Davis F 2019 Calix[4]amine Langmuir-Blodgett thin film sensing properties against volatile organic compounds *J. Phys. Conf. Ser.* **1186** 012011
[44] Durmaz M, Acikbas Y, Bozkurt S, Capan R, Erdogan M and Ozkaya C 2021 A novel calix[4]arene thiourea decorated with 2-(2-aminophenyl)benzothiazole moiety as highly selective chemical gas sensor for dichloromethane vapor *ChemistrySelect* **6** 4670–6
[45] Rathod N V, Rao A, Kumar P, Ramakumar K L and Malkhede D D 2014 Complexation with calixarenes and efficient supercritical CO_2 extraction of Pb(II) from acidic medium *New J. Chem.* **38** 5331–40
[46] Zhang L, Zhang Y, Tao H, Sun X, Guo Z and Zhu L 2002 Investigation of calix[4]arene–porphyrin and its Palladium(II) and Zinc(II) complexes at air/water interface and in Langmuir–Blodgett film *Thin Solid Films* **413** 224–30
[47] Shirshov Y M *et al* 1997 Optical parameters of thin calixarene films and their response to benzene, toluene and chloroform adsorption *Supramol. Sci.* **4** 491–4
[48] Bozkurt S, Durmaz M, Erdogan M, Ozkaya Erdogan C, Capan R and Acikbas Y 2022 The bisbenzothiazole-p-tert-butylcalix[4]arene-thiourea Langmuir–Blodgett thin films: preparation, optical properties, swelling dynamics and gas sensing properties via host–guest principles *J. Inclusion Phenom.Macrocyclic Chem.* **102** 629–36
[49] Halay E, Acikbas Y, Capan R, Bozkurt S, Erdogan M and Unal R 2019 A novel triazine–bearing calix[4]arene: design, synthesis and gas sensing affinity for volatile organic compounds *Tetrahedron* **75** 2521–8
[50] Benounis M, Jaffrezic N, Martelet C, Dumazet-Bonnamour I and Lamartine R 2015 High sensitive surface plasmon resonance (SPR) sensor based on modified calix(4)arene self assembled monolayer for cadmium ions detection *Mater. Trans.* **56** 539–44
[51] Nabok A V, Hassan A K and Ray A K 2000 Condensation of organic vapours within nanoporous calixarene thin films *J. Mater. Chem.* **10** 189–94
[52] Roales J, Pedrosa J M, Castillero P, Cano M and Richardson T H 2011 Optimization of mixed langmuir–blodgett films of a water insoluble porphyrin in a calixarene matrix for optical gas sensing *Thin Solid Films* **519** 2025–30
[53] Ozmen M, Ozbek Z, Bayrakci M, Ertul S, Ersoz M and Capan R 2014 Preparation and gas sensing properties of Langmuir–Blodgett thin films of calix[n]arenes: Investigation of cavity effect *Sensors Actuators B* **195** 156–64
[54] Acikbas Y *et al* 2017 Fabrication and characterization of calix[4]arene langmuir–blodgett thin film for gas sensing applications *J. Inclusion Phenom. Macrocyclic Chem.* **89** 77–84
[55] Bayrakcı M, Ertul Ş and Yilmaz M 2012 Phase solubility studies of poorly soluble drug molecules by using o-phosphorylated calixarenes as drug-solubilizing agents *Journal of Chemical & Engineering Data* **57** 233–9
[56] Sayin S 2022 Synthesis of new anthracene-conjugated calix[4]arene as highly selective fluorescent chemosensor for determination of CN^- ion *J. Mol. Struct.* **1252** 132212
[57] Ozkaya Erdogan C, Capan R, Acikbas Y, Ozmen M and Bayrakci M 2022 Sensor application of pyridine modified calix[4]arene Langmuir-Blodgett thin film *Optik* **265** 169492
[58] Aydin Z, Keskinates M, Yilmaz B and Bayrakci M 2023 An isonicotinohydrazide based fluorescence sensor for detection of Zn^{2+} in biological systems: experimental and theoretical studies along with cell imagine *Inorg. Chim. Acta* **557** 121680
[59] Gassoumi B, Ghalla H and Chaabane R B 2019 DFT and TD-DFT investigation of calix[4]arene interactions with $TFSI^-$ ion *Heliyon* **5** e02822
[60] Kalchenko O I *et al* 2023 Complexation of water-soluble phosphorylated calixarenes with uracils. Stability constants and DFT study of the supramolecular complexes *J. Inclusion Phenom. Macrocyclic Chem.* **103** 369–83